Available online at www.sciencedirect.com
ScienceDirect
Cement & Concrete Composites 30 (2008) 374–380
Cement & Concrete Composites
www.elsevier.com/locate/cemconcomp

Strain–temperature hysteresis in concrete under cyclic freeze–thaw conditions

Shashank Bishnoi [a,*], Taketo Uomoto [b,1]

[a] Laboratoire de Matériaux de Construction, Ecole Polytechnique Fédérale de Lausanne, EPFL-STI-IMX-LMC, Station 12, 1015 Lausanne, Switzerland
[b] Institute of Industrial Science, University of Tokyo, 4-6-1 Komaba Meguro-ku, Tokyo 153-8505, Japan

Received 8 November 2006; received in revised form 13 January 2008; accepted 14 January 2008
Available online 26 January 2008

Abstract

Submerged concrete specimens with 0.55 and 0.65 water–cement ratio were studied under cyclic freeze–thaw conditions at two different rates of temperature change. The strain variation at the centres of each of the specimens was measured using embedded strain-gauges. The strain at the centres of the specimens due to thermal gradients were modelled based only on the temperatures at the surface and the centres of the specimens. It was found that the hysteresis observed in the strain–temperature variations could be attributed to the thermal gradients with significant accuracy even at low rates of temperature change. Thermal gradients were found to be an essential requirement of any comprehensive modelling dealing with cyclic freeze–thaw tests in the laboratory.

Keywords: Cyclic freezing and thawing; Strain–temperature behaviour; Hysteresis; Strain modelling

1. Introduction

It is rather ironic that water, one of the main components of concrete responsible for its strength development, is also one of the major causes of its deterioration being associated with the various processes leading to corrosion of reinforcement and even cracking of concrete. Cyclic freeze–thaw deterioration is arguably the deterioration mechanism most directly affected by water. The case of cyclic freeze–thaw damage is complex with even the water present in the finest pores of concrete present in a half-bound state from the time the concrete was prepared, playing a role [1].

Powers [1–5] was the first to study cyclic freezing and thawing and presented a series of ground-breaking articles on possible mechanisms underlying the process and methods to quantify damage due to the process within a period of around 10 years. Powers used sample dilations as a measure of deterioration and reported that undamaged specimens exhibit higher thermal expansion coefficients at sub-zero temperatures. Despite length measurements being the traditional measure of freeze–thaw deterioration, to the authors knowledge, strain measurements, which are a natural extension of length measurements are relatively little studied. Though some attempts to characterize the strain variations have been made [6–9], no particular theory has been able to adequately explain the observed behaviour. It is, however, generally known that concrete exhibits predominantly linear contractions down to −20 °C [8] and that a hysteresis is observed in the strain–temperature behaviour [6]. Residual strains have also been shown to increase progressively with the progress of deterioration [8,10]. Still, the current understanding of strain variations in concrete is limited to a few studies highlighting the need for comprehensive work on this problem.

This study is an attempt to study the strain–temperature variations in concrete under cyclic freezing and thawing conditions from the point of view of temperature gradients. A simple analysis of thermal gradients within prismatic specimens due to the relatively low thermal diffusivity of

* Corresponding author. Tel.: +41 21 693 6859; fax: +41 21 693 5800.
E-mail address: shashank.bishnoi@epfl.ch (S. Bishnoi).
[1] Tel.: +81 3 5452 6391; fax: +81 3 5452 6392.

0958-9465/$ - see front matter © 2008 Elsevier Ltd. All rights reserved.
doi:10.1016/j.cemconcomp.2008.01.005

concrete and its effect on the hysteresis observed in the strain–temperature behaviour, has been presented. Penttala and Al-Neshawy [6] presented relations modelling this hysteresis behaviour based on the hydraulic pressures generated in the pore system of concrete and found that though the pore-pressures can lead to a hysteresis similar to that observed, the theoretically derived values deviated remarkably from those observed experimentally. The current study however neglects the effect of pore-pressures and focusses only on thermal gradients.

2. Objectives

The aim of this research is to study the hysteresis in the strain–temperature behaviour of concrete under cyclic freeze–thaw conditions down to around −25 °C and to identify the contribution of thermal gradients to the hysteresis. The experiments in the current study are limited to concretes of relatively higher water to cement ratios of 0.55 and 0.65. Simplistic relations, modelling the strains in the specimens as a function of various temperatures, are derived and then compared against experimental measurements. The results obtained clearly indicate that thermal gradients, within generally used test conditions, can contribute extensively to a hysteresis in the strain–temperature behaviour, and that, within the given test regime, most of the observed hysteresis can be attributed to the thermal gradients.

The significance of this study lies in the deduction that thermal gradients can cause considerable variation in the measured strains and that any accurate analysis of strains would require proper consideration of the thermal gradients.

3. Experimental programme

3.1. Test programme

Prismatic specimens of two sizes were subjected to rapid freeze–thaw cycles. Strain and temperature variations at the centre of the specimens were measured using embedded strain-gauges, the main variables in the experiments being specimen sizes, heating/cooling rate, water-cement ratio and air entrainment. A schematic of the experimental set-up is shown in Fig. 1. The specimens were placed inside rubber sleeves which were then placed inside a large insulated test-chamber. The test-chamber was filled with 'Ni-Brine', which is a thermal exchange fluid similar to coolants used in auto-mobiles. The temperature variations in this fluid are programmed before the start of the experiments. A continuous flow of the thermal fluid is maintained to ensure a uniform temperature throughout the test-chamber. Water was poured in the sleeves up to 1 cm over the upper surface of the specimen. A temperature gauge was inserted in each of the sleeves at around half the depth of the water and the temperature measured from this gauge was assumed to be the temperature at the surface of the specimens. All strain and temperature data

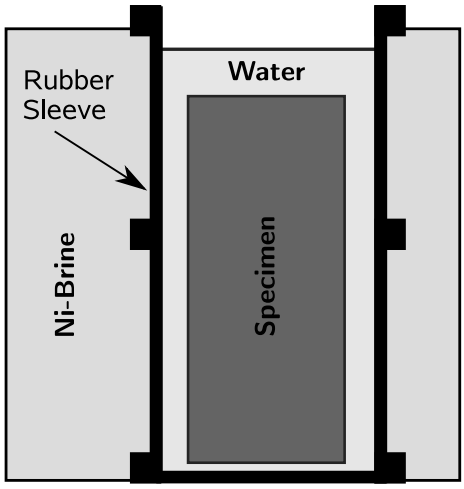

Fig. 1. Experimental set-up.

was recorded in electronic form using automatic data-loggers at 5 min intervals. The temperature of the thermal fluid was varied between 20 °C and −25 °C at two different cycle periods of 4 h (faster cycles) and 36 h (slower cycles). A total of 20 such cycles, first five of the slower type followed by 15 of the faster type were carried out. The temperature variations in the thermal fluid in a typical cycle of each type are shown in Fig. 2 along with the typical temperatures on the surface and the centres of the specimens.

3.2. Materials and mixes

Concrete was prepared using ordinary Portland cement, river sand and crushed coarse aggregate. The mix-proportions and physical properties of the concrete mixes are shown in Table 1. Fine aggregate (FA) from Fuji River, Japan, with a density of 2.63 g/cm^3 and absorption coefficient of 2.19%, was used in the mix. Crushed coarse aggregate (CA) having a maximum aggregate size of 20 mm, procured from Ryojin village in Saitama Prefecture, Japan, with a dry density of 2.73 g/cm^3 and absorption coefficient of 0.57% was used. The experiments were the part of a larger series of experiments and the relatively high water–cement ratios were used in order to achieve higher levels of deteriorations in shorter time-scales.

3.3. Specimens

This study was the part of a larger experimental programme comprising of around 50 specimens studying the general behaviour of concrete specimens of different sizes under cyclic freeze–thaw conditions. Results from only five of these specimens that were relevant to this study have been presented here. The specifications of these specimens are listed in Table 2. All specimens had embedded strain-gauges at their centres as shown in Fig. 3. The low elastic modulus and water-proof construction of these gauges makes them ideally suited for use within concrete. However, the measurements with these gauges require experimental derivation

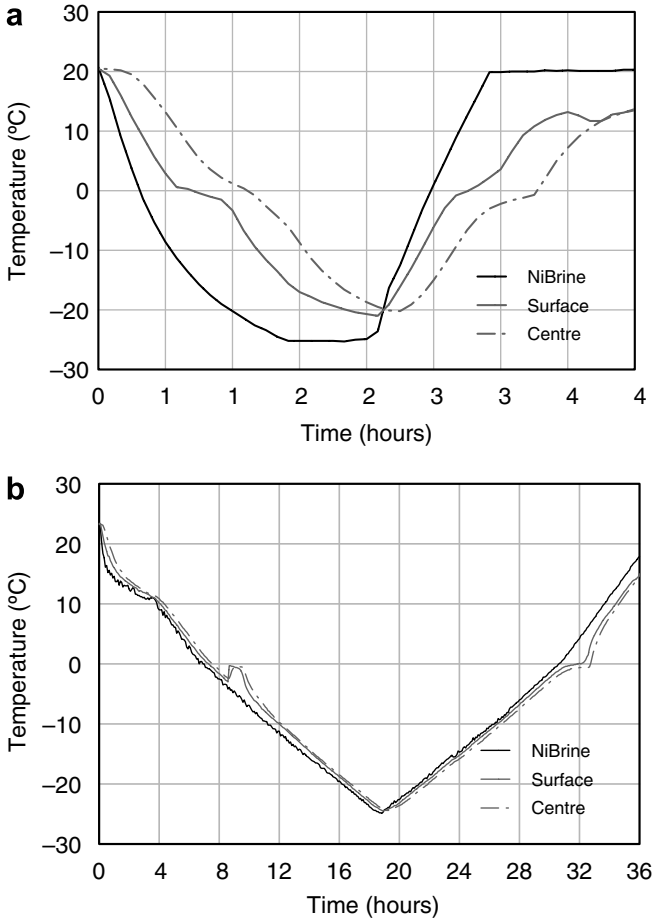

Fig. 2. Temperature variations in thermal exchange fluid, the surface and centres of specimens for (a) 4-h cycles, and (b) 36-h cycles.

Table 2
Details of specimens

S. no.	Specimen code	Mix no.	Size (cm)
1	A	I	7 × 7 × 38
2	B	I	10 × 10 × 38
3	C	I	15 × 15 × 38
4	D	II	10 × 10 × 36
5	E	III	10 × 10 × 36

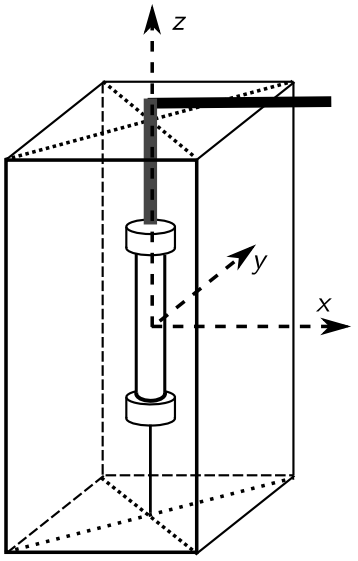

Fig. 3. Orientation of strain-gauge.

of a 'calibration factor' as is discussed in the next section. The specimens were first cured submerged under water for a total period of 15 days. At the end of these 15 days, the specimens were cushion wrapped and transported to the test-site, being removed from water for around 24 h. The specimens were then placed inside the testing chamber inside rubber sleeves, with water filled around the specimens for a period of 14 days before the freeze–thaw cycles were started. The temperature of the water around the specimens varied between 17 °C and 20 °C in this period.

4. Results and analysis

4.1. Strain–temperature behaviour

It was found that undamaged concrete contracts monotonically with the reduction of temperature down to the minimum temperature used here of −25 °C. Though expansions upon reduction of temperature have been reported [6,8], such behaviour has been observed only at temperatures lower than around −30 °C, which are beyond the scope of this study. The most easily observable feature of the strain–temperature curves obtained from the experiments was the hysteresis between the freezing and thawing paths of the strain–temperature curves. Such a hysteresis in the strain–temperature variations as has been reported earlier at high rates of temperature change [6,9]. In the current experiments, the strains measured at the same temperature were lower during freezing than during thawing. It must be noted that throughout this study, extensions in length are represented by increase in strain and reductions in length of the samples are represented by reduction in strain.

A part of the hysteresis can be attributed to the thermal gradients within the specimens. During freezing, the

Table 1
Unit(1 m^3) composition of concrete in Series 1

Mix no.	W/C ratio	Water (kg)	OPC (kg)	FA (kg)	CA (kg)	Water reducer (%)	Air entraining agent (%)	Air (%)	28 day strength (MPa)
I	0.55	160	291	826	1032	1.10	0.60	7.00	39.8
II	0.65	185	285	927	948	1.00	0.00	1.00	37.6
III	0.65	165	249	895	992	1.10	1.00	7.00	23.0

temperature at the surface of the specimen would be lower than that at the centre, thus the strain would be lower than it would have been had the specimen been at a uniform temperature, same as that at the centre. However, during thawing, the average temperature of the specimen would be higher than that at the centre giving a higher strain than in the case of uniform temperature. The strain would thus be higher during thawing than during freezing measured for the same temperature at the centre. Consistent with this, the hysteresis during slower cycles was found to be less pronounced than that observed during the faster cycles, the thermal gradients being less pronounced for lower rates of temperature change. However, given the complex boundary conditions in the tests, it is not possible to directly account for, or even estimate the order of strains induced due to thermal gradients. In the following sections, simplified relations for the hysteresis in such specimens due to thermal gradients are be derived, validated and compared against the strains observed experimentally.

4.2. Analysis of strain–temperature behaviour

Although it is possible to model the strains in prismatic specimens with defined thermal gradients using finite element method (FEM) packages, the process is time consuming and tedious. This study models the strain–temperature variations in the samples in order to simplify the calculation of temperature-dependent strains in samples with thermal gradients. As the relations depend only on the geometry of the specimens and the measured temperatures, analysis allows quick calculations of strains using a simple spreadsheet application or even manually.

Although it is known that the freeze–thaw process is a combination of various processes acting in tandem, only a basic analysis, which will later be seen to be sufficient in this case, will be presented here, considering only thermal gradients within the specimens. Pore-pressures and other hydraulic forces have been neglected.

4.2.1. Simplification of thermal gradients

In order to estimate the strain at the centre of a prismatic specimen with a square cross-section, we shall first characterize the temperature distribution in the body of the specimen in terms of the temperature at the centre and the surface. If the temperature (T) in a body changes both with time (t) and location (x, y and z, in Cartesian coordinate system), the heat transfer in the absence of a heat source inside is characterized by the well known heat equation shown below.

$$\frac{\partial T}{\partial t} = D \cdot \left(\frac{\partial^2 T}{\partial x^2} + \frac{\partial^2 T}{\partial y^2} + \frac{\partial^2 T}{\partial z^2} \right) \tag{1}$$

Where D is the thermal diffusivity of concrete. If the centre of the specimen is assumed to be the origin of the Cartesian system, it can be safely assumed that the temperature is uniform along the z axis in the vicinity of the plane $z = 0$, due to the z-dimension of the specimens being much larger than the x and y dimensions. In other words

$$\left| \frac{\partial^2 T}{\partial z^2} = 0 \right|_{z=0} \tag{2}$$

The three-dimensional problem characterized in Eq. (1) would thus be reduced to two-dimensions. We further assume the temperature to be constant throughout the surface of the specimen and a perfect symmetry about the x and y axes. Assuming the thermal contours to be running parallel to the surface of the specimen and considering the temperature variation only along the line $x = y$, the problem can be further reduced to only a single dimension as below

$$\left| \frac{\partial^2 T}{\partial x^2} = \frac{\partial^2 T}{\partial y^2} \right|_{y=x} \tag{3}$$

Thus,

$$\frac{\partial T}{\partial t} = 2D \cdot \frac{\partial^2 T}{\partial x^2} \tag{4}$$

We further assume that the rate of change of temperature varies linearly with x, thus

$$\frac{\partial^2 T}{\partial x \partial t} = \text{constant} \tag{5}$$

Assuming the rate of temperature on the surface to be $K_0(t)$ and that at the centre of the specimen $K_i(t)$, Eq. (4) can be rewritten as

$$K_i + \frac{(K_0 - K_i)}{a} \cdot 2x = 2D \cdot \frac{\partial^2 T}{\partial x^2} \tag{6}$$

Where a is the length of the side of the square cross-section of the specimen. If the temperatures at the surface ($T_0(t)$) and at the centre ($T_i(t)$) are known, Eq. (6) can be integrated twice with the application of the boundary conditions to obtain

$$T = \frac{K_i}{4D} x^2 + \frac{(K_0 - K_i)}{6aD} x^3 + \left(\frac{2(T_0 - T_i)}{a} - \frac{K_0 + 2K_i}{24D} a \right) \cdot x + T_i \tag{7}$$

Eq. (7), thus, gives the temperature distribution on the line as a function of temperatures and rates of temperature change on the surface and at the centre. Thus if the temperature variations at the centre and the surface of the specimen are known, approximate thermal gradients can be estimated.

4.2.2. Simplification of elastic strains

In order to calculate the approximate strains from these thermal gradients, we assume that the strain in the z direction is uniform throughout the xy plane at a given moment in time (Fig. 3). Though this assumption would hold for smaller specimens, as used in this study, it would not be appropriate for larger specimens, where plane

deformations are not negligible when compared to the overall deformations. The plane for which the thermal gradients have been calculated above can thus be modelled as a system of parallel elastic springs, oriented in the z direction, with equal natural lengths (l_0) at a base temperature of T_b and equal displacement (Δl) at any moment in time.

Here, a small region around the plane $z = 0$ would be considered composed of infinite concentric hollow pipes of square cross-section with cross-section area dA_i and uniform temperatures throughout each pipe. If each pipe is considered as an individual independent spring, the length of the spring at a temperature T would be

$$l_T = l_0(1 + \alpha(T - T_b)) \tag{8}$$

Where α denotes the thermal expansion coefficient of the material of the springs and is uniform for all springs. However, since a uniform strain in the z direction is assumed throughout the xy plane, all springs will have an equal length of $l_0 + \Delta l$. The total force in the springs can be calculated as the sum of elastic forces, due to the deviation of the actual length of the springs from the theoretical length at the individual temperatures of the springs (Eq. (8)):

$$\sum_i F_i = \sum_i E \cdot dA_i \cdot (l_0 + \Delta l - l_0(1 + \alpha(T_i - T_b))) = 0 \tag{9}$$

For the sake of simplicity we can assume T_b to be 0. Here the strain (ε) can be defined as $\Delta l/l_0$. Eq. (9) can thus be rewritten as

$$\sum_i dA_i(\varepsilon - \alpha T_i) = 0 \Rightarrow \sum_i dA_i\varepsilon = \sum_i dA_i\alpha T_i$$
$$\Rightarrow \varepsilon = \alpha \cdot \frac{\sum_i T_i \cdot dA_i}{A} \tag{10}$$

where A is the total cross-section area of the specimen and equals a^2. Considering an large number of elements of small size in the specimen, and replacing dA by $8x \cdot dx$, Eq. (10) can be rewritten in the integral form as

$$\varepsilon = \frac{8\alpha}{A}\int_0^{a/2} Tx\,dx \tag{11}$$

Eq. (7) can be substituted in Eq. (11) and solved to calculate ε as below

$$\varepsilon = \frac{8\alpha}{A}\left(\frac{K_i}{256D}a^4 + \frac{K_0 - K_i}{960D}a^4 + \frac{T_i}{8}a^2 + \frac{b}{24}a^3\right) \tag{12}$$

Where

$$b = \frac{2}{a}\left(T_0 - T_i - \frac{K_0 + 2K_i}{48D}a^2\right) \tag{13}$$

Using the above calculated relations, an approximate value of the strains can be calculated based only on temperature variations at the surface and the centre of the specimens. K_0 and K_i can be calculated in various ways if the variation of temperature with time is known. The strength of this method lies in obtaining quick solutions for different specimens and even upon changing material parameters for the same specimen, which would normally require repetition of the entire analysis if FEM analysis is used.

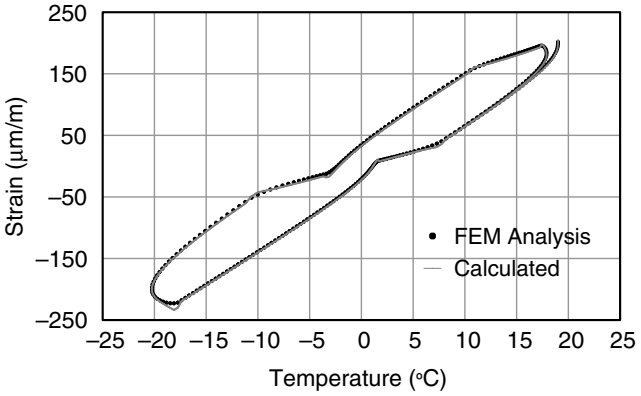

Fig. 4. Comparison of calculated values with high-resolution FEM Analysis.

4.3. Verification of the derived relation

The above derived, Eqs. (12) and (13), have been compared to a solution obtained with an FEM analysis on a sample with a fine mesh-size. The analysis was carried out using the software Ansys 6.0, using strain-analysis coupled with transient thermal analysis, with the only input being the material properties and the surface temperature. Samples of size $10 \times 10 \times 36$ cm were meshed with uniformly sized cube-elements of 0.5 cm size on each side. Quadratic elements, with all three translational degrees of freedom available at each node, were used for the analysis. The same sample and material parameters were input in both the FEM and the approximate analysis and the temperature variations used in the simulations were close to those observed in the experiments with faster cycles. The temperatures obtained from the transient-thermal analysis were used to obtain strains using the above derived relation and the values were compared to those obtained from the coupled strain–temperature analysis. The results are shown in Fig. 4. The curves were found to be in good agreement and it can be concluded that an acceptable trend of strain–temperature variations and estimates of hysteresis assuming linear-elastic conditions can be obtained using the above formulated relations.

5. Discussion

5.1. Qualitative comparison of experimental and calculated strains

The calculated strain values have been plotted along with the experimentally observed values in Figs. 5 and 6. Three consecutive cycles of the faster type and a single cycle of the slower type are plotted for each specimen. Since α and D are the only two unknowns in the derived

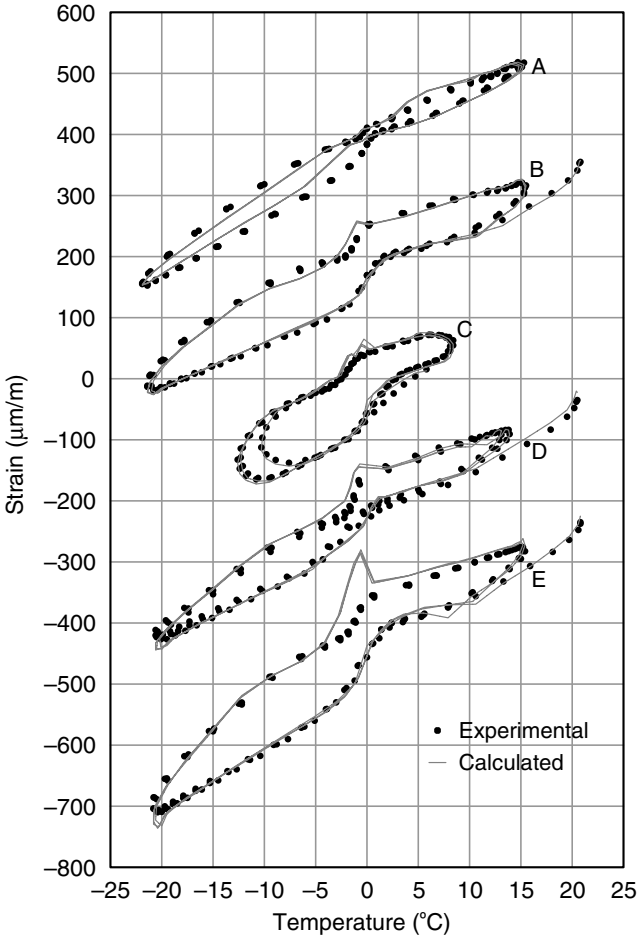

Fig. 5. Experimental and calculated strain values for 4-h cycles.

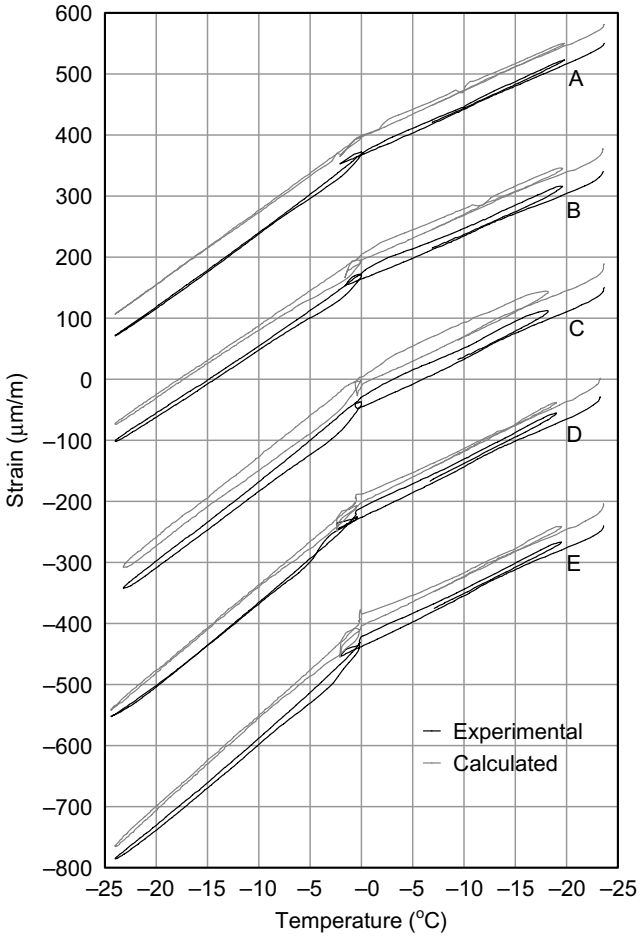

Fig. 6. Experimental and calculated strain values for 36-h cycles.

relations, these are the only two parameters that require fitting. The value of D was first fitted based on the hysteresis observed in the part of the curve over 0 °C, where it can be safely assumed that pore-pressures do not play a significant role. A significantly higher value of α was required to fit the values below 0 °C as compared to over 0 °C. This is, however, in agreement with previously reported results [4,8] where higher contraction rates in concrete were observed after freezing. The fitting was thus carried out with two different values of α for frozen and unfrozen states, depending on the temperature at the centre of the specimen. The spike in the calculated strain-values near 0 °C is induced due to this sudden change in α, the value being changed only when the temperature at the centre has reached 0 °C, regardless of the temperatures elsewhere in the specimens.

It must be noted here that for the sake of ease of representation, the strains have been normalised such that the calculated strain of specimen C at a uniform temperature of 0 °C is 0 μm/m. The strains of other specimens have been translated at intervals of 200 μm/m along the strain-axis. In Fig. 6, showing the curves for the 36-h cycles, the experimental curves have been translated downward from those calculated to ease visual observations.

Table 3
Parametric values used for fitting results

Specimen code	D (m^2/s)	α – 4 h cycles (μm/m/°C)		α – 36 h cycles (μm/m/°C)	
		Frozen	Unfrozen	Frozen	Unfrozen
A	7.27×10^{-7}	11.0	7.7	12.0	7.7
B	2.18×10^{-7}	10.0	7.5	11.2	7.5
C	2.18×10^{-7}	12.0	8.0	13.0	8.0
D	1.45×10^{-7}	11.5	8.5	14.0	8.5
E	1.45×10^{-7}	15.4	8.2	15.2	8.2

5.2. Parametric fitting

Figs. 5 and 6 show good agreements between the calculated and the experimentally measured values, with the calculated curves closely emulating the shape and the size of the experimentally observed values. A minor deviation from the experiments was however observed in the case of Specimen A, where, though the shapes being similar, the calculated hysteresis is less pronounced than that observed. The possible cause of this deviation could be the relatively larger amount of water present around the specimen leading to non-uniform boundary conditions.

However, this cannot be quantitatively verified from the current experiments.

5.2.1. Thermal expansion coefficients

The values of the parameters used for fitting the curves in Figs. 5 and 6 are listed in Table 3. The observed values of α were found to be slightly (about 15%) lower than those found in literature. Though no specific reason was found for this shift, various experimental factors, that would vary from one specimen to another, could have contributed to it. It is thus not surprising to see a small variation in the measured thermal expansion coefficients from specimens made from the same concrete. However, since this study does not make a comparison between the strains or expansion coefficients measured for different specimens, this error can be neglected. It is still possible to study the variation of strains and α in the same specimen.

It was observed that the thermal expansion coefficients in frozen states are consistently higher than those in the unfrozen state. This behaviour has been earlier attributed to the shrinkage of concrete due to the movement of water from the much finer gel pores to the capillary pores as freezing in the capillary pores takes place [10,11].

5.2.2. Thermal diffusivity

The calculated thermal diffusivity values, as shown in Table 3, were found to lie over a relatively wide range. Specially the value for specimen A is almost thrice that observed for specimens B and C, which were prepared using the same mix. While no two specimens can be expected to behave in exactly the same manner, this observation could also be attributed to the smaller size of specimen A. Although, not explicitly considered in the current study, the effect of pore-pressures might have been indirectly accounted for in the fit-values. Faster dissipation of these pore-pressures in specimen A, which has a smaller size, could explain the high observed diffusivity value. This conjecture has, however, not been investigated in more detail.

In reality, the measured hysteresis is highly sensitive to the thermal diffusivity of concrete, as thermal diffusion controls thermal gradients. However, since the temperature at the centre of the specimens was also measured in the current experiments, the possible error in the calculated strains due to an error in the diffusivity value is reduced.

6. Conclusions

The strain–temperature behaviour of concrete specimens with three different mix-proportions was presented. The most easily visible feature of the strain–temperature curves presented was the hysteresis between the freezing and thawing curves. It was shown that a significant portion of this hysteresis can be attributed to the thermal gradients generated within the specimens. Analytical relations for the calculation of strains induced due to these thermal gradients were derived using various simplifications and verified against numerically obtained results, and were compared with experimental values. The comparisons revealed that, in the current test conditions, the hysteresis can be modelled using thermal gradients with high accuracy. The thermal expansion coefficient of concrete was found to significantly increase upon freezing similar to earlier studies. The results highlight the importance of accounting for thermal gradients in mechanical experiments conducted under variable temperature conditions even at higher temperatures. Although it appears that in the current test-regime, the effects of pore-pressures are secondary to thermal gradients, it is possible that the effects of phenomenon not included in the analysis, may have been indirectly accounted for in the fitting process. This would indicate that the equations related to stresses from thermal gradients could also be utilised to model other independent phenomena that affect strain measurements in concrete under cyclic freezing and thawing conditions.

References

[1] Powers TC. The air requirements of frost-resistant concrete. In: Proceedings of the Highway Research Board. Portland Cement Association; 1949. p. 1–28.
[2] Powers TC. A working hypothesis for further studies of frost resistance of concrete. J Am Concr Soc 1945;16:245–71.
[3] Powers TC, Brownyard TC. Studies of the physical properties of hardened portland cement paste. J Am Concr I 1947;18:549–602.
[4] Powers TC, Helmuth RA. Theory of volume changes in hardened portland cement paste during freezing. In: Proceedings of Highway Research Board; 1953. p. 285–97.
[5] Powers TC. Void space as a basis for producing air-entrained concrete. J Am Concr Inst 1954;25:741–60.
[6] Penttala V, Al-Neshawy F. Stress and strain state of concrete during freezing and thawing cycles. Cem Concr Res 2002;32:1407–20.
[7] Penttala V. Freezing-induced strains and pressures in wet porous materials and especially in concrete mortars. Adv Cem Based Mater 1998;7:8–19.
[8] Miura T, Lee DH. Deformation and deterioration of concrete subjected to cyclic cooling down to very low temperatures. In: Proceedings of the National Research Council, Canada, second Canada/Japan workshop on low temperature effects on concrete; 1991. p. 23–37.
[9] Hasan M, Okuyama H, Sato Y, Ueda T. Stress–strain model of concrete damaged by freezing and thawing cycles. J Adv Concr Technol, Japan Concr Inst 2004;2:89–99.
[10] Bishnoi S. Strain variations in concrete subjected to cyclic freezing and thawing. Masters thesis, University of Tokyo, Japan; 2004.
[11] Setzer MJ. Micro-ice-lens formation in porous solid. J Colloid Interf Sci 2001;243:193–201.